This article has been accepted for inclusion in a future issue of this journal. Content is final as presented, with the exception of pagination.

Magnetic States and Bandgaps of B-Site Substituted Double-Perovskite $Ba_2Pr(Bi, Sb)O_6$

H. Taniguchi[1], M. Matsukawa[1], K. Onodera[1], K. Nishidate[1], and A. Matsushita[2]

[1]Faculty of Science and Engineering, Iwate University, Morioka 020-8551, Japan
[2]National Institute for Materials Science, Ibaraki 305-0047, Japan

We demonstrated crystal structures, magnetic, and optical properties of the B-site substituted double-perovskite $Ba_2Pr(Bi_{1-x}Sb_x)O_6$ ($x = 0$, 0.1, 0.2, 0.25, 0.3, 0.4, 0.5, and 1.0). The single-phase polycrystalline samples with the light Sb substitution are formed in a monoclinic structure (C^2/m). The heavily Sb-substituted samples crystallize in the rhombohedral system accompanied by B-site disorder. Magnetization measurements show that the effective magnetic moments are located around 3.2 μ_B for the lightly Sb-substituted samples, indicating the valence mixing between Pr^{3+} and Pr^{4+}. The magnetic moments with the heavy Sb substitution are close to the valence of Pr^{3+}. The magnitudes of bandgap energy for the two end-member samples were estimated from the optical measurements to be $E_g = 0.977$ eV at $x = 0$ and 2.395 eV at $x = 1.0$. The effect of the bandgap opening due to Sb substitution is examined by using the density functional theory. The lightly and heavily Sb-doped compounds show typical absorption edges in indirect and direct semiconductors, respectively. These findings are qualitatively consistent with the calculated results.

***Index Terms*—Density functional theory, magnetic semiconductors.**

I. Introduction

A LARGE number of double-perovskite oxides $A_2B'B''O_6$ have been widely studied due to their attractive physical properties and potential applications [1], [2]. Some of the semiconducting $A_2B'B''O_6$ compounds exhibit photocatalytic properties such as hydrogen generation by water splitting and are taken as alternative materials for TiO_2 oxide [3], [4]. In particular, Ba_2PrBiO_6 compound has been shown to possess high photocatalytic activity, which is probably related to the valence mixing [5], [6]. A previous study on the magnetic states of Ba_2PrBiO_6 compound suggests an anomalous valence situation for Pr ions [7]. The complicated ground states of rare earth ions such as Pr ion under the crystal field effect remain an open question, not only in the physical properties of the double-perovskite compound but also in the viewpoint of physics of $4f$ electron systems.

There are significant factors such as charge and size differences between B′ and B″ sites to determine the B-site ordering of the double-perovskite oxide [8]. Increase in lattice strain and/or increase in the electrostatic repulsion overcome the entropy contribution toward disordering, causing the alternate arrangement. For $A_2^{2+}B'^{3+}B''^{5+}O_6$ composition, the B-sites tend to order with increasing the ion size difference $\triangle r_B = r_{B'} - r_{B''}$. If $\triangle r_B > 0.2$ Å, it is well known that the B-sites of the compounds are almost ordered alternately in all the crystallographic axes [8]. In $Ba_2^{2+}Pr^{3+}Bi^{5+}O_6$ compound, the B-site ionic radius difference $\triangle r_B = 0.23$ Å meets the above-mentioned condition, suggesting the B-site ordering ($r_{B'}$ (Pr^{3+}) = 0.99 Å and $r_{B''}$ (Bi^{5+}) = 0.76 Å) [9].

The density functional theory-based calculation reveals the band structure and its associated orbital states of this compound and predicts the stability of crystal structures of B-site ordered states [10], [11].

In this paper, we report X-ray diffraction measurements, magnetic susceptibilities, and diffuse reflectance spectra of the $Ba_2Pr(Bi_{1-x}, Sb_x)O_6$ compounds, to determine crystal structures, magnetic, and optical properties of B-site substituted double-perovskite oxide. In [13], we have focused on the influence of light Sb substitution on crystal structures, magnetic, and optical properties in $Ba_2Pr(Bi_{1-x}, Sb_x)O_6$. It is of much interest to examine the B-site ordering of the double-perovskite oxides by substituting the smaller Sb^{5+} ion for the Bi^{5+} site, where the former and latter ions have the closed shell of $4d^{10}$ and $5d^{10}$.

II. Experiment

Polycrystalline samples of Sb-substituted Ba_2PrBiO_6 were prepared with the conventional solid-state reaction technique. The stoichiometric mixtures of $BaCO_3$, Pr_6O_{11}, Bi_2O_3, and Sb_2O_3 powders were ground, sintered in air at 800 °C–900 °C for 2 days with intermediate grindings, and pressed into pellets. The pellet samples were annealed in air at 1000 °C for 4 days. We performed X-ray diffraction measurements at room temperature with an Ultima IV diffractometer (Rigaku) using Cu-Kα radiation.

The dc magnetization was conducted at a magnetic field of 1 T under the zero-field cooling process using a superconducting quantum interference device magnetometer (Magnetic Property Measurement System, Quantum Design). Optical spectra were measured by using a diffuse reflectance method with a spectrophotometer (Hitachi U-3500) and $BaSO_4$ was used as the reference material. The optical bandgaps for the powder samples were evaluated from reflectance spectral data using the conventional Kubelka–Munk functions [7], [12]. We calculated the band structures of monoclinic Ba_2PrBiO_6 and rhombohedral Ba_2PrSbO_6 by using the density functional

Manuscript received June 5, 2018; accepted September 27, 2018. Corresponding author: M. Matsukawa (e-mail: matsukawa@iwate-u.ac.jp).

Color versions of one or more of the figures in this paper are available online at http://ieeexplore.ieee.org.

Digital Object Identifier 10.1109/TMAG.2018.2874431

0018-9464 © 2018 IEEE. Personal use is permitted, but republication/redistribution requires IEEE permission.
See http://www.ieee.org/publications_standards/publications/rights/index.html for more information.

This article has been accepted for inclusion in a future issue of this journal. Content is final as presented, with the exception of pagination.

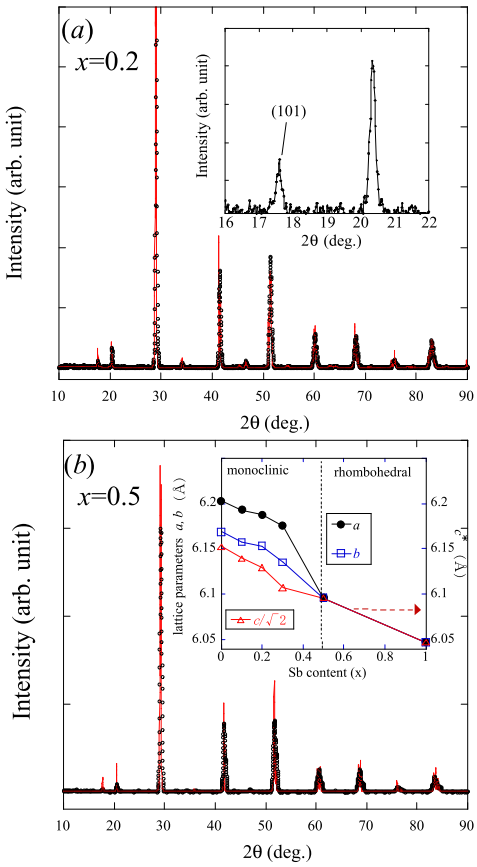

Fig. 1. (color online) X-ray diffraction patterns for (a) $Ba_2PrBi_{0.8}Sb_{0.2}O_6$ and (b) $Ba_2PrBi_{0.5}Sb_{0.5}O_6$. Insets of (a) and (b) display the enlarged diffraction profiles and the lattice parameters as a function of Sb content. The calculated profiles based on the monoclinic and rhombohedral structure models are shown in (a) and (b), respectively.

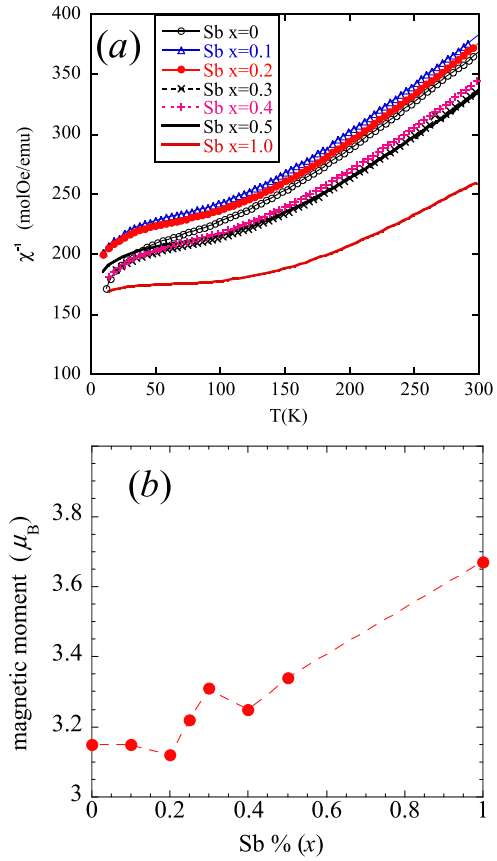

Fig. 2. (color online) (a) Inverse magnetic susceptibilities (χ^{-1}) for $Ba_2Pr(Bi_{1-x},Sb_x)$ O_6 (x = 0, 0.1 0.2, 0.3, 0.4, 0.5, and 1.0). (b) Effective magnetic moment plotted as a function of Sb content. The value of μ_{eff} is evaluated using the Curie–Weiss law.

theory as implemented in the code Vienna Ab initio Simulation Package (VASP).

III. Results and Discussion

The X-ray diffraction patterns for $Ba_2PrBi_{0.8}Sb_{0.2}O_6$ and $Ba_2PrBi_{0.5}Sb_{0.5}O_6$ are shown in Fig. 1(a) and (b), respectively. The polycrystalline samples with the lower Sb contents are formed in almost single phases with a monoclinic structure (the space group C^2/m) as shown in [7] and [13]. For the parent Ba_2PrBiO_6, the lattice parameters are $a = 6.2038$ Å, $b = 6.1689$ Å, $c = 8.7011$ Å and $\beta = 89.7303°$. The emergence of (101) reflection [the inset of Fig. 1(a)] indicates B-cation ordering, which is characteristic of the B-site ordered double-perovskite structure. The substitution of the smaller Sb^{5+} (0.60 Å) ion at the Bi^{5+} (0.76 Å) site causes a monotonic decrease in the lattice parameters as displayed in the inset of Fig. 1(b). The heavily Sb-substituted samples with $x = 0.5$ and 1.0 crystallize in a rhombohedral structure with the space group $R\bar{3}$. For the Ba_2PrSbO_6, the lattice parameters $a = 6.04671$ Å and $\alpha = 60.1646°$ are estimated from the X-ray diffraction data using RIETAN-FP program, which are in good agreement with previous data [14], [15]. In Fig. 1(b), the corresponding (101) peak observed at the $x = 0.2$ sample is strongly suppressed at $x = 0.5$, indicating the B-site disordering.

The inverse magnetic susceptibilities (χ^{-1}) for $Ba_2Pr(Bi_{1-x},Sb_x)$ O_6 (x = 0, 0.1 0.2, 0.3, 0.4, 0.5, and 1.0) are shown in Fig. 2(a) as a function of temperature at a magnetic field of 1 T. All measured samples show no signature of magnetic ordering over a wide range of temperatures. The low-temperature magnetic behavior in the parent Ba_2PrBiO_6 is well described by the crystal field effect of the Pr ion [6]. From the magnetization data at high temperatures above 200 K, we estimate the effective magnetic moment according to the Curie–Weiss law. The value of effective magnetic moment μ_{eff} is evaluated by using the following formula:

$$C = N\mu_{\text{eff}}^2\mu_B^2/3k_B$$

where C, N, and μ_B denote the Curie constant, the number of magnetic atom per mol, and the Bohr magneton, respectively. Performing the calculation for the end member samples, we obtained that $\mu_{\text{eff}} = 3.15$ and 3.67 μ_B in the $x = 0$ and $x = 1.0$ cases, respectively. As shown in Fig. 2(b), the magnetic moment is almost stable at low-Sb content, then it shows a gradual increase upon increasing the Sb content and finally reaches ~3.6 μ_B. Next, we try to estimate the ratio of Pr^{3+} and Pr^{4+} using the following:

$$\mu_{\text{eff}}^2 = y\mu_{\text{eff}}^2(Pr^{3+}) + (1-y)\mu_{\text{eff}}^2(Pr^{4+})$$

This article has been accepted for inclusion in a future issue of this journal. Content is final as presented, with the exception of pagination.

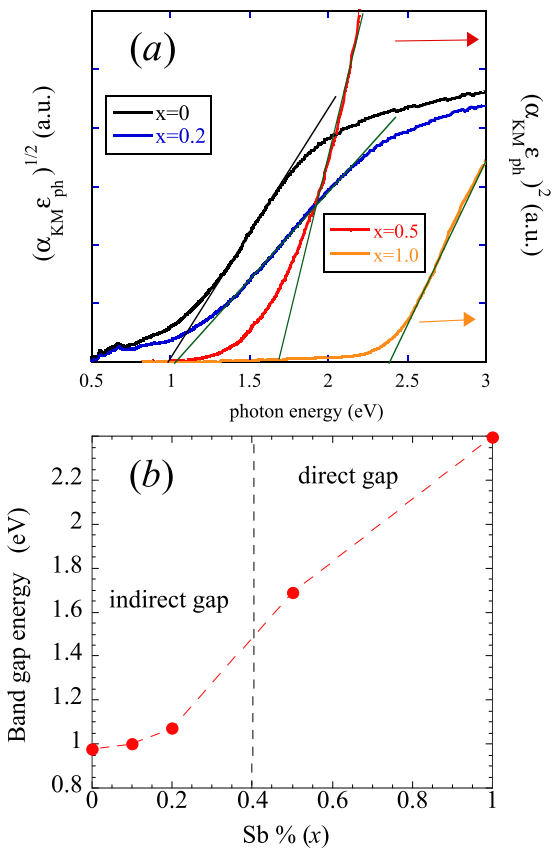

Fig. 3. (color online) Optical properties of $Ba_2Pr(Bi_{1-x}, Sb_x)$ O_6 ($x = 0$, 0.2, 0.5, and 1.0). (a) Plots of $(\alpha_{KM}\varepsilon_p)^{1/2}$ versus ε_p and $(\alpha_{KM}\varepsilon_p)^2$ versus ε_p. Straight lines: extrapolations to estimate the bandgaps using the least square method. (b) Bandgap energy versus Sb content. We evaluate $E_g = 0.977$ eV at $x = 0$ and 2.395 eV at $x = 1.0$, assuming indirect and direct energy gaps, respectively.

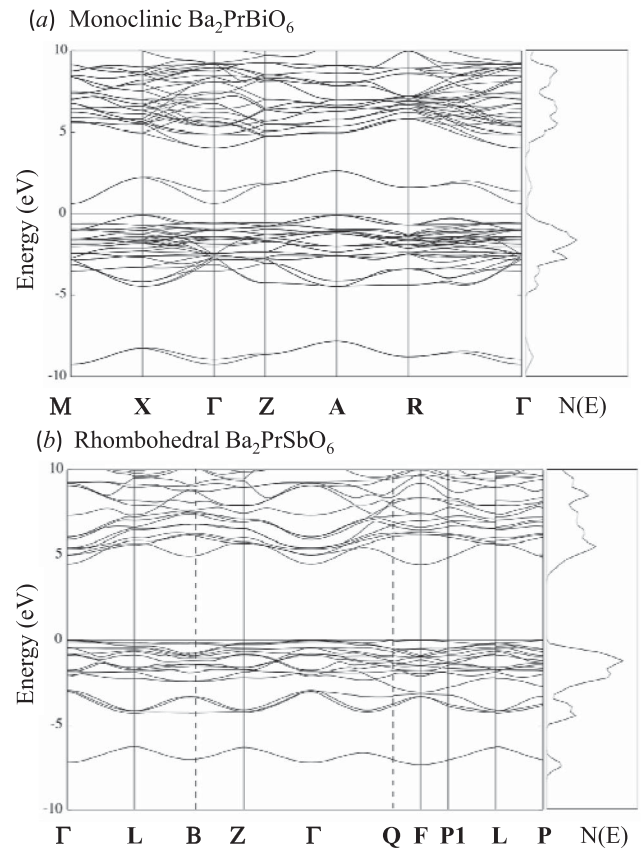

Fig. 4. Energy band structures and total density of states calculated by the density functional theory for (a) Ba_2PrBiO_6 and (b) Ba_2PrSbO_6 compounds. Bandgaps are estimated to be ~ 0.62 and 4.42 eV, for the parent monoclinic and rhombohedral compounds, respectively.

where $\mu_{\text{eff}}(Pr^{3+}) = 3.58\ \mu_B$ and $\mu_{\text{eff}}(Pr^{4+}) = 2.54\ \mu_B$. For the parent sample, the ratio of Pr^{3+} and Pr^{4+} (y:$1-y$) is 0.55: 0.45. When Sb content is increased up to 0.5, the ratio of Pr^{3+} ($\sim$0.75) becomes more dominant than that of Pr^{4+}. For the end member $x = 1.0$, we expect that Pr ions almost exist as the trivalent state. The X-ray photoemission spectroscopy analysis of the parent sample [13] revealed that a prominent peak of Pr^{3+} is dominant with a smaller shoulder structure of Pr^{4+}, which is consistent with the mixed valence state of Pr ion.

We demonstrate the optical properties for $Ba_2Pr(Bi_{1-x},Sb_x)$ O_6 ($x = 0$, 0.2, 0.5, and 1.0) powder samples measured by the diffuse reflectance method. First, the observed reflectance data for the powder samples are transformed to the absorption coefficient α_{KM} by using the conventional Kubelka–Munk function. Next, for the Kubelka–Munk conversion data near the band edge, we extrapolate the tangent line to the ε_p-axis and evaluate the optical bandgaps from the intersection according to the equation of

$$(\alpha_{KM}\varepsilon_p)^n \propto (\varepsilon_p - E_g)$$

where α_{KM}, ε_p, and E_g are the absorption coefficient, the photon energy, and the bandgap energy [5], [6]. Here, the power exponent n on the left-hand side of the above-mentioned formula depends on the types of photon transition of optical absorption. For direct and indirect bandgaps, we assume that $n = 2$ and $n = 1/2$ [5], [6]. The optical measurements determine whether the gap is direct or indirect. Fig. 3(a) shows the absorption coefficient as a function of photon energy. For the $x = 0$ and $x = 0.2$ samples, we adopt $(\alpha_{KM}\varepsilon_p)^{1/2}$ versus ε_p plot. The square of the absorption coefficient for the $x = 0.5$ and $x = 1.0$ samples, $(\alpha_{KM}\varepsilon_p)^2$, is plotted as a function of ε_p. We estimate $E_g = 0.977$ eV at $x = 0$ and 2.395 eV at $x = 1.0$, assuming indirect and direct photon transitions, respectively. Straight lines denote the extrapolations to estimate the bandgaps using the least square method. The magnitude of the energy bandgap is substantially enhanced with increasing the Sb content. When the Sb content exceeds 50%, the nature of photon absorption is changed from the indirect to direct transitions.

Finally, the effect of the bandgap opening by the atomic substitution is examined by our first-principles electric structure calculation. In Fig. 4, we have calculated the band structure of monoclinic Ba_2PrBiO_6 and rhombohedral Ba_2PrSbO_6 by using the density functional theory as implemented in the code VASP [10], [11], [16]. For monoclinic Ba_2PrBiO_6, the energy gap is determined to be an indirect transition type because the valence and conduction band edges are located at different points of X and Γ. The magnitude of its bandgap is evaluated

This article has been accepted for inclusion in a future issue of this journal. Content is final as presented, with the exception of pagination.

to be about 0.62 eV at the parent Ba_2PrBiO_6, which is quite smaller than the observed value (0.98 eV). The underestimation of the calculated bandgap in the parent monoclinic compound is probably related to strongly electron correlation not to consider in our research. On the other hand, in the case of rhombohedral Ba_2PrSbO_6 [Fig. 4(b)], we clearly predict a direct transition type of bandgap with $E_g = 4.4$ eV that is not so far from the observed value (=∼2.4 eV). The discrepancy in the magnitude of bandgap seems to be influenced by the B-site disordering of the highly Sb-substituted samples. A previous study [12] on BaBiO perovskite oxide predicts that the 6 s orbitals of the Bi atom occupy a large portion of both valence and conduction bands, forming a narrow bandgap of this compound. The B-site Sb substitution for Bi causes a reduction of the Bi orbitals and then results in the enlarged bandgaps. We believe that these findings are closely related to its variation from the indirect to direct transitions.

IV. Conclusion

In this paper, we synthesized the single-phase powder samples of $Ba_2Pr(Bi_{1-x}Sb_x)\ O_6$ by means of the Sb substitution for the Bi sites. The X-ray diffraction data revealed that the polycrystalline samples with low Sb contents crystallize in a monoclinic structure. For the heavily Sb substitution, the rhombohedral structure is stable, but the (101) reflection is strongly suppressed, indicating the B-site disordering.

Furthermore, we investigated the magnetic and optical properties of the B-site substituted perovskite oxides. The effective magnetic moment for the lightly Sb-substituted samples, 3.2 μ_B, indicates the valence mixing between Pr^{3+} and Pr^{4+}. For the heavy Sb substitution, the value of the magnetic moment is close to the valence of Pr^{3+}. The optical spectra were measured using a diffuse reflectance method. For the two end-member samples, we evaluated from the plots of the absorption coefficient versus the photon energy, the indirect and direct energy gap energies, $E_g = 0.977$ eV at $x = 0$ and 2.395 eV at $x = 1.0$. Finally, the effect of Sb substitution on the energy bandgap was examined by using the density functional theory. The Sb substitution for the Bi sites causes a substantial reduction of the Bi orbitals and then results in the enhanced bandgap. We believe that these findings are closely related to its variation from the indirect to direct transitions.

Acknowledgment

This work was supported by a research grant from The Mazda Foundation.

References

[1] K.-I. Kobayashi, T. Kimura, H. Sawada, K. Terakura, and Y. Tokura, "Room-temperature magnetoresistance in an oxide material with an ordered double-perovskite structure," *Nature*, vol. 395, p. 677, Oct. 1998.

[2] R. Ramesh and N. A. Spaldin, "Multiferroics: Progress and prospects in thin films" *Nature Mater.*, vol. 6, no. 1, pp. 21–29, 2007.

[3] A. Fujishima and K. Honda, "TiO_2 photoelectrochemistry and photocatalysis," *Nature*, vol. 238, no. 5358, pp. 37–38, 1972.

[4] H. W. Eng, P. W. Barnes, B. M. Auerand, and P. M. Woodward, "Investigations of the electronic structure of d^0 transition metal oxides belonging to the perovskite family," *J. Solid State Chem.*, vol. 175, no. 1, pp. 94–109, 2003.

[5] T. Hatakeyama *et al.*, "Photocatalytic activities of Ba_2RBiO_6 (R=La, Ce, Nd, Sm, Eu, Gd, Dy) under visible light irradiation," *J. Ceram. Soc. Jpn.*, vol. 118, no. 1374, pp. 91–95, 2010.

[6] A. Matsushita, T. Nakane, T. Naka, H. Isago, Y. Yamada, and Y. Yamada, "Valence states of rare-Earth ions and band gaps in $RBiBa_2O_6$ (R=La, Ce, Pr, Nd, Sm, Gd, Eu, and Dy) photocatalysts," *Jpn. J. Appl. Phys.*, vol. 51, pp. 121802-1–121802-5, Nov. 2012.

[7] T. A. William Harrison, K. P. Reis, A. J. Jacobson, L. F. Schneemeyer, and J. V. Waszczak, "Syntheses, structures, and magnetism of barium/rare-Earth/bismuth double perovskites. Crystal structures of Ba_2MBiO_6 (M=Ce, Pr, Nd, Tb, Yb) by powder neutron diffraction," *Chem. Mater.*, vol. 7, pp. 2161–2167, Nov. 1995.

[8] S. Vasala and M. Karppinen, "$A_2B'B'O_6$ perovskites: A review," *Prog. Solid State Chem.*, vol. 43, pp. 1–36, May 2015.

[9] R. D. Shannon, "Revised effective ionic radii and systematic studies of interatomic distances in halides and chalcogenides," *Acta. Crystallogr.*, vol. A32, pp. 751–767, Sep. 1976.

[10] G. Kresse and J. Hafner, "*Ab initio* molecular dynamics for liquid metals," *Phys. Rev. B, Condens. Matter*, vol. 47, pp. 558–561, Jan. 1993.

[11] G. Kresse and J. Furthmuller, "Efficient iterative schemes for *ab initio* total-energy calculations using a plane-wave basis set," *Phys. Rev. B, Condens. Matter*, vol. 54, pp. 11169–11186, Oct. 1996.

[12] J. W. Tang, Z. G. Zou, and J. H. Ye, "Efficient photocatalysis on $BaBiO_3$ driven by visible light," *J. Phys. Chem. C*, vol. 111, no. 34, pp. 12779–12785, 2007.

[13] K. Onodera *et al.*, "Magnetic, thermodynamic and optical properties of Sb-substituted Ba_2PrBiO_6 double perovskite oxides," *J. Phys. Conf. Ser.*, vol. 969, no. 1, pp. 012122-1–012122-6, 2018.

[14] W. T. Fu and D. J. W. Ijdo, "X-ray and neutron powder diffraction study of the double perovskites Ba_2LnSbO_6 (Ln=La, Pr, Nd and Sm)," *J. Solid State Chem.*, vol. 178, pp. 2363–2367, Jul. 2005.

[15] S. Otsuka and Y. Hinatsu, "Structures and magnetic properties of rare Earth double perovskites containing antimony or bismuth Ba_2LnMO_6 (Ln=rare Earths; M=Sb, Bi)," *J. Solid State Chem.*, vol. 227, pp. 132–141, Jul. 2015.

[16] K. Nishidate, N. Yoshimoto, P. Chantngarm, H. Saito, and M. Hasegawa, "Tuning the work function of graphene with the adsorbed organic molecules: First-principles calculations," *Mol. Phys.*, vol. 114, no. 20, pp. 2993–2998, 2016.